

Article

Hydrothermal Extraction and Characterization of Cellulose Fibers from Bamboo Moso (*Phyllostachys edulis*) Culms

Andrea Marangon ^{1,2,*} , Elisa Calà ^{1,2} , Alessandro Bessi ¹ , Alessandro Croce ³ , Enrico Avattaneo ⁴, Eleonora Cara ⁵  and Giorgio Gatti ^{1,2} 

¹ Dipartimento per lo Sviluppo Sostenibile e la Transizione Ecologica, Università degli Studi del Piemonte Orientale, Piazza S. Eusebio 5, 13100 Vercelli, Italy

² GEA G.S. s.r.l.s., Piazza S. Eusebio 5, 13100 Vercelli, Italy

³ SSD Research Laboratories, Research and Innovation Department (DAIRI), Azienda Ospedaliero-Universitaria SS. Antonio e Biagio e Cesare Arrigo, Via Venezia 16, 15121 Alessandria, Italy

⁴ Lisante Service S.r.l., Viale Europa 25, 15053 Castelnuovo Scrivia, Italy

⁵ Advanced Materials and Life Science Division, Istituto Nazionale di Ricerca Metrologica, Strada delle Cacce 91, 10135 Torino, Italy

* Correspondence: andrea.marangon@uniupo.it

Highlights

What are the main findings?

- The delignification of bamboo was carried out using a hydrothermal process in the presence of a weak base such as NH_4OH at different treatment times. The characterisation of the delignified materials showed that, after just 3 h of treatment, the amount of lignin present had decreased compared to the original material.

What are the implications of the main finding?

- The main implication of this work is that it demonstrates how it is possible to produce delignified material from whole bamboo culms using dilute solutions of weak bases, with shorter processing times than those currently in use.

Abstract

In recent years, there has been a notable increase in commercial demand for natural fibers. Consequently, numerous studies have concentrated on formulating innovative industrial production methodologies for natural fibers, with a particular emphasis on the environmental sustainability of production processes. Among natural fiber sources, bamboo has emerged as a leading candidate, attracting considerable interest due to its exceptional renewability, rapid growth, and low cultivation requirements. The contemporary industrial methodologies employed in the extraction of cellulose from bamboo frequently entail the utilization of concentrated solutions of strong acids and bases, often at elevated temperatures and with extended treatment durations. These processes generate highly polluting waste from mineral acids and bases, posing significant environmental challenges and ecosystem damage. In response to the prevailing concerns, there has been a marked increase in the focus on environmentally friendly techniques that combine enzymatic treatments, selective chemical reagents, and optimized mechanical processes. These processes facilitate the extraction of high-quality bamboo fibers, which are suitable for utilization in the textile industry and have the potential to replace synthetic fibers. This work demonstrates the efficacy of methodologies employing more diluted solutions than conventional approaches. Specifically, this study utilizes a weak base, such as NH_4OH , in conjunction with hydrothermal



Academic Editor: Martin J. D. Clift

Received: 23 December 2025

Revised: 7 March 2026

Accepted: 13 March 2026

Published: 20 March 2026

Copyright: © 2026 by the authors.

Licensee MDPI, Basel, Switzerland.

This article is an open access article distributed under the terms and

conditions of the [Creative Commons Attribution \(CC BY\)](https://creativecommons.org/licenses/by/4.0/) license.

extraction. It is therefore possible for dilute weak base solutions to yield natural fibers after a relatively brief period of processing, typically just a few hours.

Keywords: bamboo fiber extraction; hydrothermal extraction; cellulose fiber characterization

1. Introduction

Research in the textile sector is constantly evolving to identify new extraction methods and plant sources that minimize the environmental impact of natural textile fibers [1]. New plant materials for textile fiber production have also been extensively evaluated [2]. In recent years, efforts to enhance bamboo fibers have driven progress due to their distinctive properties, including high mechanical strength, antibacterial and antifungal activity, UV light absorption, and remarkable softness [3–6]. Bamboo fiber application in the textile industry offers notable advantages in terms of eco-sustainability, as it is both biodegradable and renewable within a short period [5,7,8]. This is attributed to the rapid growth rate of the bamboo plant, which serves as a vital economic resource in various Asian countries [9,10]. Interest in bamboo fiber stems not only from its inherent properties but also from the ecological sustainability of the plant itself. Bamboo culms are particularly effective at absorbing carbon dioxide from the atmosphere and remediating soil pollutants, especially heavy metals such as lead, arsenic, cadmium, zinc, and copper [9,11–13]. Additionally, bamboo requires less water and pesticide treatments compared with traditional natural fibers, such as cotton, hemp, and flax [14–16]. In light of the growing emphasis on sustainable industrial processes in recent years, innovative approaches have been explored to produce bamboo fibers with increased focus on environmental sustainability [17]. Current methodologies for manufacturing bamboo fibers intended for textile applications or composites predominantly rely on chemical, mechanical, or enzymatic processes [3,18–21]. These techniques require substantial water and chemical reagent consumption, generating considerable waste volumes that pose management challenges and incur disposal costs. The main processes for extracting cellulose from plant matrices such as flax, hemp, and sisal involve mineral acids and strong bases (e.g., NaOH) as an initial step to hydrolyze the lignin matrix in which cellulose fibers are embedded. The hydrolyzed material is then cooked to solubilize the hemicellulose fractions and subsequently bleached. This final treatment, typically using oxidizing agents such as H₂O₂, sodium citrate, or ozone, increases the purity of the extracted cellulose. All these steps generate large quantities of process waste [22,23]. For these reasons, research is increasingly focusing on developing new methods for extracting cellulose from plant biomass that are more sustainable than current approaches [24–26]. Chemical methods for extracting cellulose from bamboo exploit hydrolysis reactions generated by lignin reacting with OH[−] or H₃O⁺ ions, breaking the β-O-4 bond [27,28]. For the lignin hydrolysis and hemicellulose solubilization during cellulose extraction, various bases have been used, such as NaOH, KOH, and NH₃ [29–31].

The green approach to lignin solubilization, using ionic liquids, enzymes, and deep eutectic solvents, requires initial studies to design optimal combinations [32]. For these reasons, such reagents remain limited to laboratory-scale production at present.

Moreover, many bamboo procedures transform extracted cellulose into viscose [8]. Viscose production employs solutions with high concentrations of bases and organic sulfur-containing solvents [33]. This process generates significant waste that is difficult to eliminate and poses health and environmental risks, despite recent innovations that have reduced environmental impacts. Proposed novel methods use mechanical or enzymatic processes to reduce both solution volumes and reagent concentrations [34]. Over time, pioneering

chemical techniques have also been developed, employing lower reagent concentrations to produce cellulose and viscose from various sources, including bamboo and wood from softwood, hardwood, cotton linter, and hemp [7,9].

This study investigated how combining a weak-base solution, such as NH_4OH , with a hydrothermal process influences lignin hydrolysis and $\beta\text{-O-4}$ bond breakage. These findings demonstrate that NH_4OH , when paired with hydrothermal treatment, yields processable material after just a few hours, offering potential for industrial-scale optimization.

2. Materials and Methods

Bamboo (*Phyllostachys edulis*) stalks used in this work were sourced from Lisante Service s.r.l. (Castelnuovo Scrivia, Italy). All culms were dehydrated, cut into strips (7.0 ± 0.5 cm), and weighed. For all experiments, samples of 37 ± 5 g were treated with 50 mL of 10% (*v/v*) NH_4OH solution (VWR International, CAS number 1336-21-6, Radnor, PA, USA) in an autoclave. The solution with bamboo stalks was heated to 170°C for 3–24 h to determine the minimum time required for stalk defibrillation. The selected temperature of 170°C was optimized for delignification of woody materials in previous work [35].

Each test was repeated 5 times to assess reproducibility and the effects of parameters such as culm thickness, age, and part on the defibrillation process.

The materials obtained after hydrothermal extraction were separated from the solutions by filtration and immersed in 250 mL of diluted (1:50 *v/v*) hydrochloric acid (Merk, Darmstadt, Germany, CAS number 7647-01-0) to neutralize the residual base. Samples were then thoroughly rinsed with deionized water until the pH was neutral. Materials were dried in an oven at 50°C to a constant weight, allowing calculation of the weight loss percentage due to defibrillation, as reported in Table 1. A schematic of the process is shown in Figure 1.

Table 1. Mass yield of samples after hydrothermal cellulose extraction.

Time of Treatment [h]	Mass Yield [%]
3	53.5 ± 3.1
6	52.4 ± 0.4
12	42.9 ± 6.6
24	50.5 ± 7.2

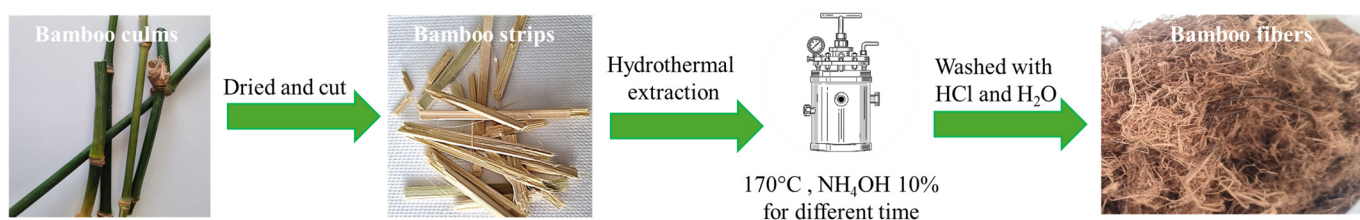


Figure 1. Diagram of the process from bamboo culms to extracted cellulose.

Scanning electron microscopy (SEM) analyses were performed with a field-emission-gun (FEG) SEM (FEI INSPECT F, Thermo Fisher Scientific, Waltham, MA, USA). Samples were gold-coated (5 nm) using a magnetron sputter coater (Cressington 108auto, Angstrom Engineering Inc., Cambridge, ON, Canada) before being loaded into the high-vacuum chamber to enable imaging despite their non-conductive surfaces. Imaging was performed at a 10 kV accelerating voltage with a 3.5 spot size and 10 mm of working distance; micrographs were acquired in top and cross-section views to visualize surface morphology.

Attenuated Total Reflectance Infrared (ATR-FTIR) analyses were performed using a Nicolet iS50 IR spectrometer (Thermo Fisher Scientific, Waltham, MA, USA), with 64 scans at a resolution of 4 cm^{-1} over the $4000\text{--}400\text{ cm}^{-1}$ range.

Thermogravimetric analyses (TGAs) were conducted using a Setaram LABSYS evo instrument (Caluire, France) equipped with differential thermal analysis (DTA) and differential scanning calorimetry (DSC) capabilities. Analyses were run under nitrogen (50 mL/min flow), from 30 to $700\text{ }^{\circ}\text{C}$ at $5\text{ }^{\circ}\text{C/min}$; 10 mg of sample was analyzed per TGA run.

X-ray diffraction (XRD) analysis was performed using an Empyrean X-ray diffractometer (Malvern Panalytical, Malvern, UK) with a Cu source (40 kV , 40 mA). Samples were scanned over $2\theta = 5\text{--}70^{\circ}$ at $3^{\circ}/\text{min}$, with Soller (0.04 rad), anti-scatter (P7.5), beam mask (10 mm), divergence ($1/4^{\circ}$), and axial ($1/2^{\circ}$) slits.

All samples were characterized using SEM, ATR-FTIR, TGA, and XRD to evaluate lignin removal efficacy from bamboo culms.

3. Results

All materials were characterized both before and after delignification with 10% (v/v) NH_4OH to assess changes in the structure and composition of the bamboo stems. The delignification process aims to break down lignin, which binds cellulose chains, thereby improving the fiber's workability. Samples of defibered material were compared with their untreated counterparts to identify differences in the percentage composition of lignin, hemicelluloses, and cellulose after delignification.

3.1. Scanning Electron Microscopy (SEM)

SEM analysis was performed to evaluate differences in sample morphology after delignification. During the process, lignin, hemicellulose, and short-chain cellulose were solubilized, while long-chain cellulose remained in the solid phase. SEM was used to verify cellulose microfibril adhesion in the samples after delignification. Figure 2 shows images of the samples before and after delignification.

The raw bamboo sample (Figure 2A) before delignification showed cellulose microfibrils emerging from a compact matrix. These fibers were not distinguishable from the surrounding matrix, with only those near fracture surfaces protruding from the compact material. Materials treated for different delignification times exhibited distinct surface morphologies. After 3 h (Figure 2B), partial emergence of cellulose microfibrils from the lignin matrix was observed, with the surface remaining compact and showing only partial lignin removal. Figure 2C,D show the materials after 6 and 12 h of delignification treatment, respectively. In these cases, delignification progressed, rendering cellulose microfibrils distinguishable from each other. Specifically, Figure 2C reveals separated cellulose fibers; however, after 6 h of treatment, these cellulose microfibrils were very short and unsuitable for the final application. In contrast, samples after 12 h of treatment exhibited distinguishable cellulose microfibrils, though in an aggregated form. Finally, samples after 24 h (Figure 2E) showed the same morphology as those after 12 h , with individual fibers no longer separated but aggregated.

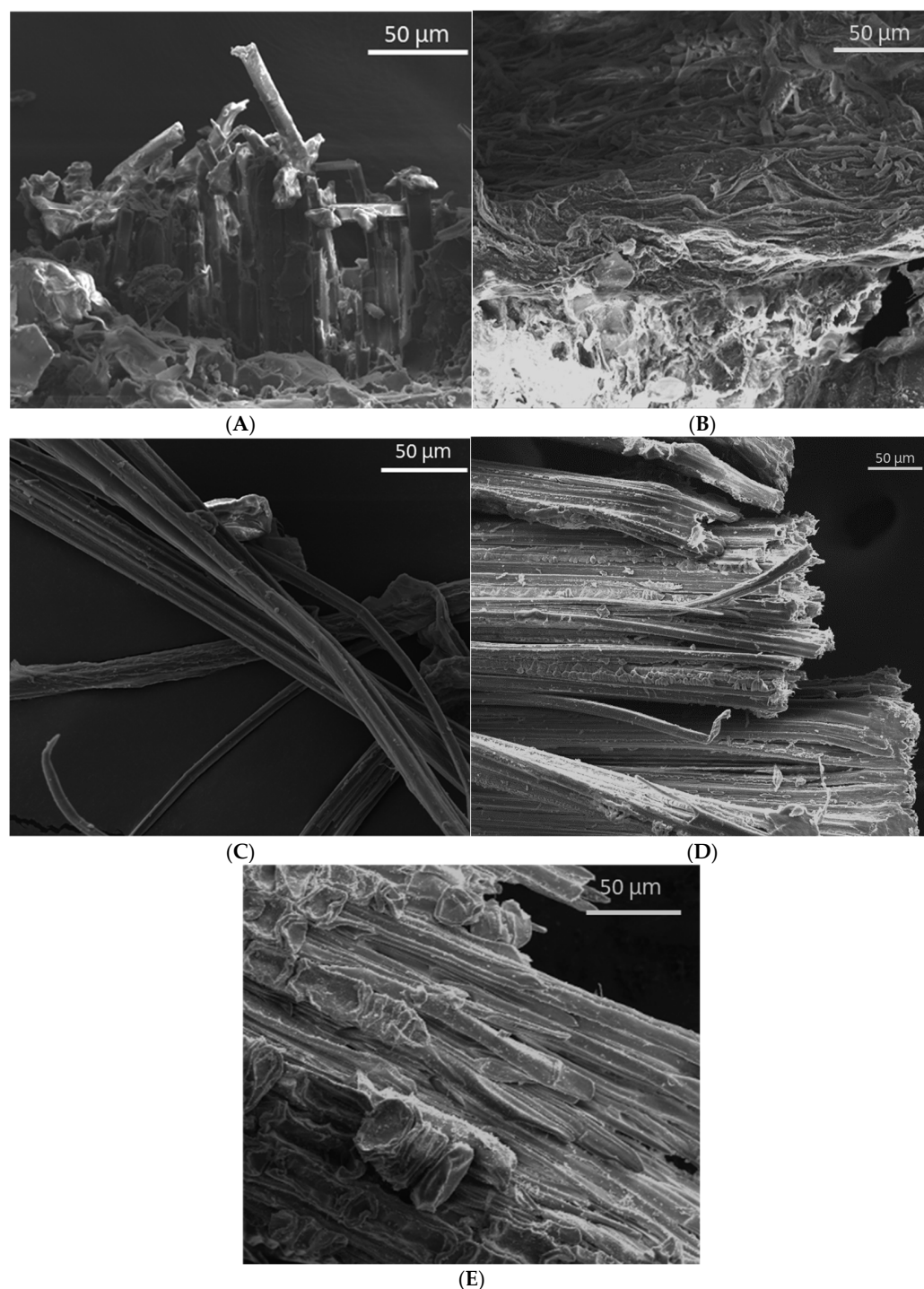


Figure 2. SEM images of the raw bamboo samples (A) after 3 h (B), 6 h (C), 12 h (D), and 24 h (E) of delignification treatment.

3.2. Infrared Spectroscopy in Total Attenuated Reflectance (ATR-FTIR)

Infrared spectroscopy in the attenuated total reflectance mode is widely used for surface analysis of materials, particularly for characterizing wood and lignocellulosic substrates [36,37]. This approach allows direct evaluation of interactions between cellulose chains and lignin within the material, as well as the determination and quantification of cellulose and lignin content [37–39]. The FTIR characterization of bamboo strips is well documented and was instrumental in identifying and assigning the peaks observed in the ATR-FTIR spectra of the bamboo samples analyzed in this study [40–43]. The spectra of the bamboo samples, shown in Figure 3, display clear changes after treatment

at 170 °C at a 10% concentration at different times. Figure 3 shows the spectra of the materials after 3 (spectra b), 6 (spectra c), 12 (spectra d), and 24 h (spectra e), in addition to the untreated bamboo (spectra a). The peaks modified by treatments are highlighted relative to the untreated material.

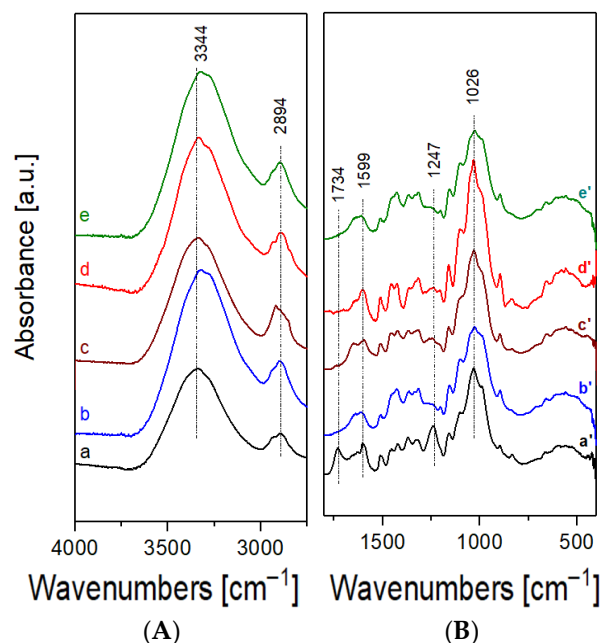


Figure 3. The ATR-FTIR spectra in the high-frequency region (A) and low-frequency region (B) show the untreated bamboo (a and a'), as well as samples treated with 10% NH_4OH solution at 170 °C for 3 h (b and b'), 6 h (c and c'), 12 h (d and d'), and 24 h (e and e').

The ATR-FTIR spectra reveal significant differences between untreated bamboo and samples subjected to delignification treatments. In the high-frequency region ($4000\text{--}2750\text{ cm}^{-1}$), the most prominent peak, associated with hydroxyl group vibrations in cellulose chains, shifted progressively toward lower wavenumbers with increasing treatment duration. Similarly, in the low-frequency region, certain peaks observed in untreated bamboo diminished after only a few hours of treatment. These spectral changes indicate structural and chemical modifications in sample composition. Compared to the original samples, bamboo samples defibered for varying durations exhibited peaks that either disappeared or shifted during the defibering process. The peaks that diminished after delignification corresponded to those at 1734 and 1247 cm^{-1} . These peaks were attributable, respectively, to stretching vibrations of unconjugated aldehyde or ketone $\text{C}=\text{O}$ groups in lignin and hemicellulose structures (the former associated with lignin), as well as to CO-OR stretching in hemicelluloses or C-O bond stretching in lignin monomer units [44]. The spectral peaks observed at 3344 , 2894 , 1599 , and 1026 cm^{-1} were assigned to stretching vibrations of hydroxyl groups in cellulose, C-H bonds in cellulose and residual lignin, $\text{C}=\text{C}$ bonds associated with unsaturated lignin structures, and in-plane C-H deformation of lignin aromatic rings and symmetric C-O stretching in cellulose and hemicelluloses, respectively [44]. All stretching modes and their corresponding wavenumbers are summarized in Table 2. The ATR-FTIR spectra, due to the decrease in signals at 1734 and 1247 cm^{-1} , indicated that a significant portion of the lignin and hemicellulose present in the original bamboo was removed during the defibration process. Nevertheless, residual lignin fragments and hemicellulose chains remained detectable in the material, albeit at reduced levels, even after 24 h of treatment.

Table 2. Assignment of the peaks in ATR-FTIR spectra.

Frequency [cm^{-1}]	Vibration Stretching Mode (ν)
3344	$\nu\text{O-H}$
2894	$\nu\text{C-H}$
1734	$\nu\text{C=O}$ unconjugated aldehydes or ketones
1599	$\nu\text{C=C}$ in lignin unsaturations
1247	$\nu\text{CO-OR}$ in hemicellulose $\nu\text{C-O}$ in the guaiacyl units of lignin
1026	$\nu\text{C-O}$

3.3. Thermogravimetric Analysis (TGA)

Thermogravimetric analyses were carried out to semi-quantitatively evaluate the presence of hemicelluloses and lignin in the materials after defibering treatment. Thermogravimetric analysis has been widely used for the characterization of plant biomass and the determination of its components based on the different degradation temperatures of cellulose, hemicellulose, and lignin [45–49]. Cellulose, hemicellulose, and lignin exhibited distinct thermal degradation ranges, which enabled confirmation of hemicellulose and lignin in the lignified materials [50]. The thermograms of the analyzed samples and their first derivatives are presented in Figure 4.

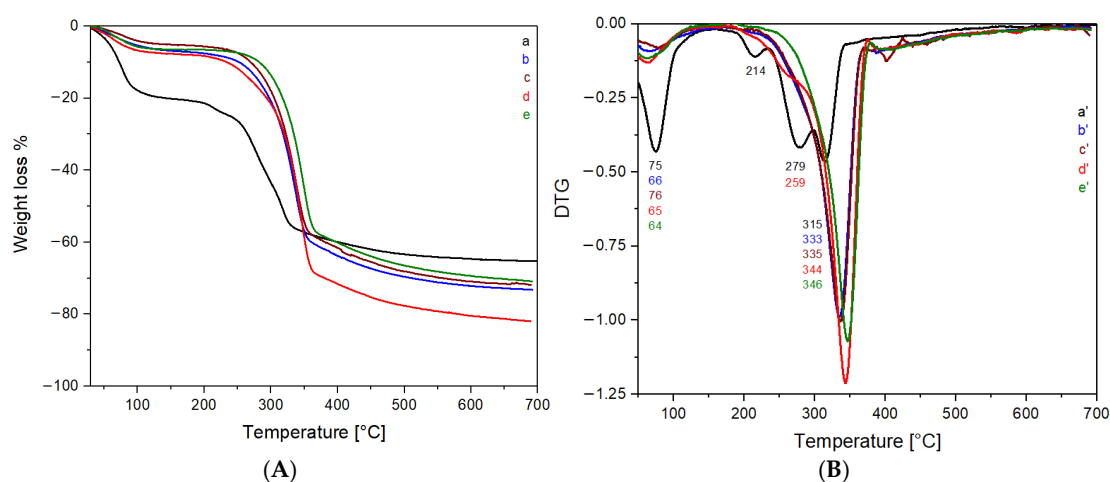


Figure 4. Thermogravimetric profile (A) and the first-derivative curves (B) of untreated bamboo (a and a') and samples treated with 10% NH_4OH at 170 °C for 3 h (b and b'), 6 h (c and c'), 12 h (d and d'), and 24 h (e and e').

Figure 4 shows the thermal profiles of the defibred samples compared with the untreated bamboo, highlighting a clear alteration in the curves after treatment, both in their shape and the disappearance of some weight loss events present in the untreated material. After comparison of the thermograms of the defibred bamboo samples, the profiles appeared very similar to one another, whereas they differed markedly from that of the original sample. All curves exhibited an initial weight loss between 65 and 80 °C, attributable to the loss of physisorbed water and volatile compounds, which was particularly pronounced in the untreated bamboo due to the presence of residual hydrated tissues [51,52]. In the untreated bamboo sample, two distinct weight loss events occurred between 200 and 275 °C, which were not observed in the defibred samples, a behavior likely related to the degradation of free sugars and hemicelluloses that were solubilized in the basic solution during the defibering process. The most significant weight loss occurred

between 300 and 350 °C, attributed to the thermal degradation of cellulose [35,51,52]. In the untreated bamboo samples, this weight loss event had an intensity comparable to that associated with hemicelluloses, whereas after 3 h of the process, it appeared to be the only major degradation step in the defibered samples. No appreciable weight loss was observed in the thermal range between 360 and 600 °C (typical of lignin thermal decomposition range) in the defibered materials, indicating a reduced lignin content after the defibering process [52]. These results suggest that both hemicellulose and a substantial fraction of lignin were removed from the materials within the first 3 h of treatment. The corresponding weight loss percentages at the relevant degradation temperatures are reported in Table 3. The data shown in Table 3 indicate that the sample treated for 12 h showed significantly greater weight loss in the temperature range between 150 and 400 °C when compared to the other samples analyzed. This was linked to greater removal of lignin and hemicellulose from the material. It is well known in the literature that prolonged treatments not only cause lignin hydrolysis reactions but also condensation reactions that lead to lignin repolymerization [53,54].

Table 3. The temperature and corresponding weight loss percentages for untreated bamboo (0) were compared with those of samples treated with 10% NH₄OH at 170 °C for durations of 3 h (3), 6 h (6), 12 h (12), and 24 h (24), respectively. This comparison highlights how increasing treatment time alters the material's thermal degradation behavior.

Time of Treatment [h]	Weight Loss %			Residual Mass % at 700 °C
	30–150 °C	150–400 °C	400–700 °C	
0	20	40	5	35
3	6	57	10	27
6	5	57	9	29
12	8	63	11	18
24	7	53	10	30

3.4. X-Ray Diffraction (XRD)

X-ray diffraction (XRD) is widely used to characterize cellulose-based materials. Determining crystallinity and structural variations in cellulose is essential during processing and extraction, as such changes can affect the mechanical properties of final materials.

Figure 5 shows diffractograms of delignified samples at different processing times.

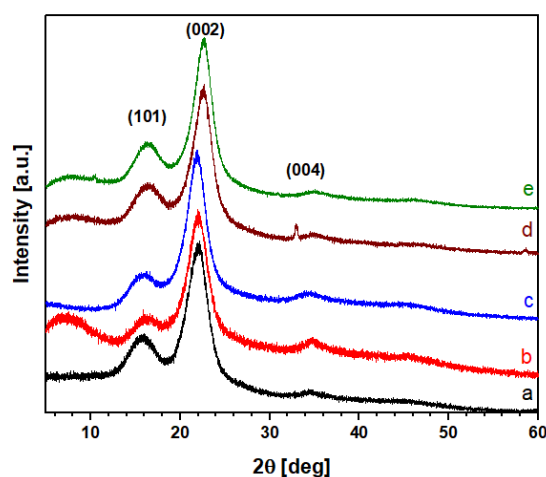


Figure 5. X-Ray diffraction pattern of raw (a) and bamboo fibers after 3 h (b), 6 h (c), 12 h (d), and 24 h (e) of delignification process.

The diffractograms of the analyzed samples (Figure 5) showed variation in the (002) reflection angle. This shift was absent for the (101) reflection, which occurred at $2\theta = 17^\circ$ across all samples. The intensity of the (004) reflection decreased with increasing process time. These angular variations indicated changes in crystallinity and cellulose chain conformation within the materials. Table 4 lists the crystallinity indices (CrI%) for the extracted cellulose samples, calculated per literature methods using Segal Equation (1) [55], shown below.

$$\text{CrI}\% = \frac{(I_{(002)} - I_{am})}{I_{(002)}} \cdot 100 \quad (1)$$

The CrI% values in Table 4 show that the crystallinity of extracted cellulose increased during the initial processing hours. This rise was directly linked to reduced lignin and hemicellulose content, as these formed amorphous fractions. The trend was consistent across the analyzed samples, except for the 12 h sample, where crystallinity decreased before rising again at 24 h.

Table 4. CrI% calculated for the samples treated at different times of the process.

Time of Treatment [h]	CrI%
0	80.5
3	85.3
6	86.1
12	83.4
24	87.9

4. Discussion

Traditional methods for bamboo processing rely on strong bases at high concentrations, hazardous solvents, large volumes of water, and extended treatment times. This study explored a more sustainable alternative using a weaker base than those typically employed in the industry. A reduction in lignin was already evident after the first 3 h of treatment at 170°C in 10% NH_4OH , but it was not sufficient to obtain a sufficiently delignified material. This possibility was observed for treatment times of at least 6 h. The characterizations were qualitatively and semi-quantitatively assessed for changes in the content of lignin, hemicellulose, and cellulose.

SEM images reveal surface modifications and cellulose microfibril aggregation post-treatment: samples after 6 h exhibited the smallest fiber dimensions and lowest workability, whereas those treated beyond 6 h showed lignin re-polymerization with cellulose fibers in an aggregated form. ATR-FTIR spectra confirm that peaks associated with lignin and hemicelluloses started to disappear after the first 3 h, with no major differences observed among spectra from 3, 6, 12, and 24 h treatments, indicating early breakdown and solubilization of these components.

Thermogravimetric analyses of the materials reveal notable differences in sample composition relevant to this study's objectives. After delignification treatment, the thermograms showed significantly lower water content compared to the untreated material. Moreover, between 300 and 350°C , the delignified samples exhibited a much steeper weight loss profile, indicating markedly lower hemicellulose concentrations and a substantial reduction in lignin content; the degradation peak related to cellulose thermal degradation appeared more pronounced.

XRD analyses reveal progressive increases in material crystallinity following the delignification. This was directly linked to reduced amorphous fractions of hemicellulose

and lignin in the analyzed materials. Crystallinity rose with longer hydrothermal treatment times, except for in the 12 h sample, which exhibited the lowest value among all the analyzed samples.

5. Conclusions

This work aimed to minimize the material/solution ratio and solution concentration used for cellulose fiber extraction from bamboo culms. Using a diluted solution of a weak base—such as NH_4OH —in combination with a hydrothermal process has the potential to allow a lignin hydrolysis reaction. The materials obtained after the delignification process were characterized. Lignin depolymerization and subsequent solubilization in aqueous solution were evident after the first few hours of treatment. SEM images show the morphological modification after the initial hours of treatment. Cellulose aggregates could be distinguished from each other; FTIR spectra show how the lignin-related bands at 1734 and 1247 cm^{-1} appeared, after the hydrothermal extraction process, to be less intense compared with the original bamboo material, indicating in a semi-quantitative way the decrease in lignin concentration in the extracted materials. Also, the thermogravimetric analysis shows a difference between the materials after different times of treatment in the temperature ranges of 200–280 °C and 365–600 °C, where, respectively, hemicellulose and lignin thermal degradation occurred, indicating a difference in terms of concentration % of the different fractions. X-ray diffraction analysis shows a progressive increase in the crystallinity of the materials subsequent to the delignification process, indicating a concomitant decrease in the concentration of lignin and hemicellulose. The data collected suggest that 12 h of hydrothermal extraction at 170 °C with 10% *v/v* of NH_4OH solutions is the compromise between lignin residual concentration and extracted cellulose yield.

Author Contributions: Conceptualization, A.M., E.C. (Elisa Calà), A.B., E.A. and G.G.; methodology, A.M., E.C. (Elisa Calà), A.B. and E.A.; validation, A.M., E.C. (Elisa Calà), A.B., E.A. and G.G.; formal analysis, A.M., A.B., E.C. (Eleonora Cara) and G.G.; resources, E.A. and G.G.; data curation, E.C. (Elisa Calà) and A.C.; writing—original draft preparation, A.M., E.C. (Elisa Calà), A.C. and G.G.; writing—review and editing, A.M., E.C. (Elisa Calà), A.B., A.C., E.A., E.C. (Eleonora Cara) and G.G.; supervision, G.G.; project administration, G.G.; funding acquisition, E.A. All authors have read and agreed to the published version of the manuscript.

Funding: This research was funded by Lisante Service s.r.l.

Data Availability Statement: The data presented in this study are available on request from the corresponding author.

Acknowledgments: Part of this work was carried out at Nanofacility Piemonte INRiM, a laboratory supported by the “Compagnia di San Paolo” Foundation, and at QR Laboratories, INRiM, a micro nanofabrication lab.

Conflicts of Interest: The authors, Andrea Marangon, Elisa Calà and Giorgio Gatti, are founding partners of the spin-off company GEA G.S. s.r.l.s. Author Enrico Avattaneo was employed by the company Lisante Service S.r.l. The remaining authors declare that the research was conducted in the absence of any commercial or financial relationships that could be construed as a potential conflict of interest. The authors declare that this study received funding from Lisante Service s.r.l. The funder was not involved in the study design, collection, analysis, interpretation of data, the writing of this article or the decision to submit it for publication.

References

1. Subash, M.C.; Muthiah, P. Eco-Friendly Degumming of Natural Fibers for Textile Applications: A Comprehensive Review. *Clean. Eng. Technol.* **2021**, *5*, 100304. [[CrossRef](#)]
2. Islam, S.U.; Shahid, M.; Mohammad, F. Perspectives for Natural Product Based Agents Derived from Industrial Plants in Textile Applications—A Review. *J. Clean. Prod.* **2013**, *57*, 2–18. [[CrossRef](#)]
3. Rocky, B.P.; Thompson, A.J. Production of Natural Bamboo Fibers-1: Experimental Approaches to Different Processes and Analyses. *J. Text. Inst.* **2018**, *109*, 1381–1391. [[CrossRef](#)]
4. Sarkar, A.K.; Appidi, S. Single Bath Process for Imparting Antimicrobial Activity and Ultraviolet Protective Property to Bamboo Viscose Fabric. *Cellulose* **2009**, *16*, 923–928. [[CrossRef](#)]
5. Bao, H.; Hong, Y.; Yan, T.; Xie, X.; Zeng, X. A Systematic Review of Biodegradable Materials in the Textile and Apparel Industry. *J. Text. Inst.* **2024**, *115*, 1173–1192. [[CrossRef](#)]
6. Mishra, R.; Behera, B.K.; Pada Pal, B. Novelty of Bamboo Fabric. *J. Text. Inst.* **2011**, *103*, 320–329. [[CrossRef](#)]
7. Thyavihalli Girijappa, Y.G.; Mavinkere Rangappa, S.; Parameswaranpillai, J.; Siengchin, S. Natural Fibers as Sustainable and Renewable Resource for Development of Eco-Friendly Composites: A Comprehensive Review. *Front. Mater.* **2019**, *6*, 226. [[CrossRef](#)]
8. Nayak, L.; Mishra, S.P. Prospect of Bamboo as a Renewable Textile Fiber, Historical Overview, Labeling, Controversies and Regulation. *Fash. Text.* **2016**, *3*, 2. [[CrossRef](#)]
9. Gratani, L.; Crescente, M.F.; Varone, L.; Fabrini, G.; Digiulio, E. Growth Pattern and Photosynthetic Activity of Different Bamboo Species Growing in the Botanical Garden of Rome. *Flora—Morphol. Distrib. Funct. Ecol. Plants* **2008**, *203*, 77–84. [[CrossRef](#)]
10. Dlamini, L.C.; Fakudze, S.; Makombe, G.G.; Muse, S.; Zhu, J. Bamboo as a Valuable Resource and Its Utilization in Historical and Modern-Day China. *BioResources* **2021**, *17*, 1926–1938. [[CrossRef](#)]
11. Dlamini, L.C.; Bian, F.; Zhong, Z.; Zhang, X.; Yang, C.; Gai, X. Bamboo—An Untapped Plant Resource for the Phytoremediation of Heavy Metal Contaminated Soils. *Chemosphere* **2020**, *246*, 125750. [[CrossRef](#)]
12. Bian, F.; Zhong, Z.; Zhang, X.; Li, Q.; Huang, Z. Bamboo-Based Agroforestry Changes Phytoremediation Efficiency by Affecting Soil Properties in Rhizosphere and Non-Rhizosphere in Heavy Metal-Polluted Soil (Cd/Zn/Cu). *J. Soils Sediments* **2023**, *23*, 368–378. [[CrossRef](#)]
13. Liang, Z.; Kovács, G.P.; Gyuricza, C.; Neményi, A. Potential Use of Bamboo in the Phytoremediation in of Heavy Metals: A Review. *Acta Agrar. Debr.* **2022**, *1*, 91–97. [[CrossRef](#)] [[PubMed](#)]
14. Zhou, X.; Guan, F.; Zhang, X.; Li, C.; Zhou, Y. Response of Moso Bamboo Growth and Soil Nutrient Content to Strip Cutting. *Forests* **2022**, *13*, 1293. [[CrossRef](#)]
15. Lin, S.; Wang, Q.; Wei, K.; Zhao, X.; Tao, W.; Sun, Y.; Su, L.; Deng, M. Comprehensive Assessment of Combined Inorganic and Organic Fertilization Strategies on Cotton Cultivation: Implications for Sustainable Agriculture. *J. Sci. Food Agric.* **2024**, *104*, 8456–8468. [[CrossRef](#)]
16. Manian, A.P.; Cordin, M.; Pham, T. Extraction of Cellulose Fibers from Flax and Hemp: A Review. *Cellulose* **2021**, *28*, 8275–8294. [[CrossRef](#)]
17. Asmare, F.W.; Liu, X.; Qiao, G.; Li, R.; Babu K, M.; Wu, D. Investigation and Application of Different Extraction Techniques for the Production of Finer Bamboo Fibres. *Adv. Bamboo Sci.* **2024**, *7*, 100070. [[CrossRef](#)]
18. Rocky, B.P.; Thompson, A.J. Production and Modification of Natural Bamboo Fibers from Four Bamboo Species, and Their Prospects in Textile Manufacturing. *Fibers Polym.* **2020**, *21*, 2740–2752. [[CrossRef](#)]
19. Amjad, A.I. Bamboo Fibre: A Sustainable Solution for Textile Manufacturing. *Adv. Bamboo Sci.* **2024**, *7*, 100088. [[CrossRef](#)]
20. Tong, X.; He, Z.; Zheng, L.; Pande, H.; Ni, Y. Enzymatic Treatment Processes for the Production of Cellulose Nanomaterials: A Review. *Carbohydr. Polym.* **2023**, *299*, 120199. [[CrossRef](#)]
21. Lobregas, M.O.S.; Buniao, E.V.D.; Leão, J.L. Alkali-Enzymatic Treatment of Bambusa Blumeana Textile Fibers for Natural Fiber-Based Textile Material Production. *Ind. Crops Prod.* **2023**, *194*, 116268. [[CrossRef](#)]
22. Chopra, L.; Manikanika. Extraction of Cellulosic Fibers from the Natural Resources: A Short Review. *Mater. Today Proc.* **2022**, *48*, 1265–1270. [[CrossRef](#)]
23. Khan, R.; Jolly, R.; Fatima, T.; Shakir, M. Extraction Processes for Deriving Cellulose: A Comprehensive Review on Green Approaches. *Polym. Adv. Technol.* **2022**, *33*, 2069–2090. [[CrossRef](#)]
24. Firouzi, M.; Siddiqua, S.; Kazemian, H.; Kiamahalleh, M.V. Green Solvent-Based Extraction of Cellulose from Hemp Bast Fibers: From Treatment Efficacy to Characterizations and Optimization. *Int. J. Biol. Macromol.* **2025**, *288*, 138689. [[CrossRef](#)] [[PubMed](#)]
25. Xia, Z.; Li, J.; Zhang, J.; Zhang, X.; Zheng, X.; Zhang, J. Processing and Valorization of Cellulose, Lignin and Lignocellulose Using Ionic Liquids. *J. Bioresour. Bioprod.* **2020**, *5*, 79–95. [[CrossRef](#)]
26. Roy, R.; Rahman, M.S.; Amit, T.A.; Jadhav, B. Recent Advances in Lignin Depolymerization Techniques: A Comparative Overview of Traditional and Greener Approaches. *Biomass* **2022**, *2*, 130–154. [[CrossRef](#)]

27. Nagel, E.; Zhang, C. Hydrothermal Decomposition of a Lignin Dimer under Neutral and Basic Conditions: A Mechanism Study. *Ind. Eng. Chem. Res.* **2019**, *58*, 18866–18880. [[CrossRef](#)]
28. Zhai, Q.; Yang, S.; Zhao, S.; Hu, J.; Lu, Y.; Zhang, X. Fractionation of Poplar Wood with Different Acid Hydrotropes: Lignin Dissolution Behavior and Mechanism Evaluation. *Int. J. Biol. Macromol.* **2023**, *253*, 126696. [[CrossRef](#)]
29. Terzopoulou, P.; Vouvoudi, E.C.; Achilias, D.S. Delignification as a Key Strategy for Advanced Wood-Based Materials: Chemistry, Delignification Parameters, and Emerging Applications. *Forests* **2025**, *16*, 993. [[CrossRef](#)]
30. Oruganti, R.K.; Sunar, S.L.; Panda, T.K.; Shee, D.; Bhattacharyya, D. Kraft Lignin Recovery from De-Oiled Jatropha Curcas Seed by Potassium Hydroxide Pretreatment and Optimization Using Response Surface Methodology. *Bioresour. Technol. Rep.* **2023**, *23*, 101572. [[CrossRef](#)]
31. Zhao, C.; Shao, Q.; Chundawat, S.P.S. Recent Advances on Ammonia-Based Pretreatments of Lignocellulosic Biomass. *Bioresour. Technol.* **2020**, *298*, 122446. [[CrossRef](#)] [[PubMed](#)]
32. Liu, E.; Mercado, M.I.V.; Segato, F.; Wilkins, M.R. A Green Pathway for Lignin Valorization: Enzymatic Lignin Depolymerization in Biocompatible Ionic Liquids and Deep Eutectic Solvents. *Enzym. Microb. Technol.* **2024**, *174*, 110392. [[CrossRef](#)]
33. Gondhalekar, S.C.; Pawar, P.J.; Dhumal, S.S.; Thakre, S. Fate of CS₂ in Viscose Process: A Chemistry Perspective. *Cellulose* **2022**, *29*, 1451–1461. [[CrossRef](#)]
34. Forsberg, D.C.R.; Bengtsson, J.; Hollinger, N.; Kaldéus, T. Towards Sustainable Viscose-to-Viscose Production: Strategies for Recycling of Viscose Fibres. *Sustainability* **2024**, *16*, 4127. [[CrossRef](#)]
35. Gullo, F.; Marangon, A.; Croce, A.; Gatti, G.; Aceto, M. From Natural Woods to High Density Materials: An Ecofriendly Approach. *Sustainability* **2023**, *15*, 2055. [[CrossRef](#)]
36. Sharma, A.; Garg, S.; Sharma, V. ATR-FTIR Spectroscopy and Machine Learning for Sustainable Wood Sourcing and Species Identification: Applications to Wood Forensics. *Microchem. J.* **2024**, *200*, 110467. [[CrossRef](#)]
37. Rana, R.; Langenfeld-Heyser, R.; Finkeldey, R.; Polle, A. FTIR Spectroscopy, Chemical and Histochemical Characterisation of Wood and Lignin of Five Tropical Timber Wood Species of the Family of Dipterocarpaceae. *Wood Sci. Technol.* **2010**, *44*, 225–242. [[CrossRef](#)]
38. Kostyukov, S.G.; Matyakubov, H.B.; Masterova, Y.Y.; Kozlov, A.S.; Pryanichnikova, M.K.; Pynenkov, A.A.; Khlyuchina, N.A. Determination of Lignin, Cellulose, and Hemicellulose in Plant Materials by FTIR Spectroscopy. *J. Anal. Chem.* **2023**, *78*, 718–727. [[CrossRef](#)]
39. Åkerholm, M.; Salmén, L. Interactions between Wood Polymers Studied by Dynamic FT-IR Spectroscopy. *Polymer* **2001**, *42*, 963–969. [[CrossRef](#)]
40. Biswas, S.; Rahaman, T.; Gupta, P.; Mitra, R.; Dutta, S.; Kharlyngdoh, E.; Guha, S.; Ganguly, J.; Pal, A.; Das, M. Cellulose and Lignin Profiling in Seven, Economically Important Bamboo Species of India by Anatomical, Biochemical, FTIR Spectroscopy and Thermogravimetric Analysis. *Biomass Bioenergy* **2022**, *158*, 106362. [[CrossRef](#)]
41. Yu, H.; Gui, C.; Ji, Y.; Li, X.; Rao, F.; Huan, W.; Li, L. Changes in Chemical and Thermal Properties of Bamboo after Delignification Treatment. *Polymers* **2022**, *14*, 2573. [[CrossRef](#)] [[PubMed](#)]
42. Yang, H.; Lin, H.; Yang, C.; Hu, H.; Dong, H.; Liu, Y.; Liu, X.; Cui, J.; Xiao, Y. Structural Regulation of Carbon Materials through Hydrothermal Mixing of Biomass and Its Application in Supercapacitors. *J. Energy Storage* **2024**, *83*, 110688. [[CrossRef](#)]
43. Chen, Q.; Ma, X.; Li, J.; Huang, H.; Cao, S.; Huang, L. Enhancing the Selective Separation of Hemicelluloses from Cellulosic Fibers in NaOH/ZnO Aqueous Solution. *Wood Sci. Technol.* **2023**, *57*, 375–387. [[CrossRef](#)]
44. Chen, C.; Luo, J.; Qin, W.; Tong, Z. Elemental Analysis, Chemical Composition, Cellulose Crystallinity, and FT-IR Spectra of Toona Sinensis Wood. *Monatsh. Chem.* **2014**, *145*, 175–185. [[CrossRef](#)]
45. Moustaqim, M.E.; Kaihal, A.E.; Marouani, M.E.; Men-La-Yakhaf, S.; Taibi, M.; Sebbahi, S.; Hajjaji, S.E.; Kifani-Sahban, F. Thermal and Thermomechanical Analyses of Lignin. *Sustain. Chem. Pharm.* **2018**, *9*, 63–68. [[CrossRef](#)]
46. Gonzalez, M.; Pereira-Rojas, J.; Villanueva, I.; Agüero, B.; Silva, I.; Velasquez, I.; Delgado, B.; Hernandez, J.; Rodriguez, G.; Labrador, H.; et al. Preparation and Characterization of Cellulose Fibers from Meghatyrsus Maximus: Applications in Its Chemical Derivatives. *Carbohydr. Polym.* **2022**, *296*, 119918. [[CrossRef](#)] [[PubMed](#)]
47. D’Acerno, F.; Michal, C.A.; MacLachlan, M.J. Thermal Stability of Cellulose Nanomaterials. *Chem. Rev.* **2023**, *123*, 7295–7325. [[CrossRef](#)]
48. Werner, K.; Pommer, L.; Broström, M. Thermal Decomposition of Hemicelluloses. *J. Anal. Appl. Pyrolysis* **2014**, *110*, 130–137. [[CrossRef](#)]
49. Brebu, M.; Vasile, C. Thermal Degradation of Lignin—A Review. *Cellul. Chem. Technol.* **2010**, *44*, 353–363.
50. Sebio-Puñal, T.; Naya, S.; López-Beceiro, J.; Tarrío-Saavedra, J.; Artiaga, R. Thermogravimetric Analysis of Wood, Holocellulose, and Lignin from Five Wood Species. *J. Therm. Anal. Calorim.* **2012**, *109*, 1163–1167. [[CrossRef](#)]
51. Ornaghi, H.L.; Ornaghi, F.G.; Neves, R.M.; Monticeli, F.; Bianchi, O. Mechanisms Involved in Thermal Degradation of Lignocellulosic Fibers: A Survey Based on Chemical Composition. *Cellulose* **2020**, *27*, 4949–4961. [[CrossRef](#)]

52. Rubiyah, M.H.; Melethil, K.; Varghese, S.; Kurian, M.; Babu, S.; Jojo, L.; Thomas, B. Isolation and Characterization of Cellulose Nanofibrils from Agro-Biomass of Jackfruit (*Artocarpus heterophyllus*) Rind, Using a Soft and Benign Acid Hydrolysis. *Carbohydr. Polym. Technol. Appl.* **2023**, *6*, 100374. [[CrossRef](#)]
53. Pei, Z.; Liu, X.; Chen, J.; Wang, H.; Li, H. Research Progress on Lignin Depolymerization Strategies: A Review. *Polymers* **2024**, *16*, 2388. [[CrossRef](#)] [[PubMed](#)]
54. Sen, S.; Patil, S.; Argyropoulos, D.S. Thermal Properties of Lignin in Copolymers, Blends, and Composites: A Review. *Green Chem.* **2015**, *17*, 4862–4887. [[CrossRef](#)]
55. Segal, L.; Creely, J.J.; Martin, A.E.; Conrad, C.M. An Empirical Method for Estimating the Degree of Crystallinity of Native Cellulose Using the X-Ray Diffractometer. *Text. Res. J.* **1959**, *29*, 786–794. [[CrossRef](#)]

Disclaimer/Publisher’s Note: The statements, opinions and data contained in all publications are solely those of the individual author(s) and contributor(s) and not of MDPI and/or the editor(s). MDPI and/or the editor(s) disclaim responsibility for any injury to people or property resulting from any ideas, methods, instructions or products referred to in the content.